HEMOGLOBIN-CARBON MONOXIDE BINDING RATE

LOW TEMPERATURE MAGNETO-OPTICAL DETECTION OF SPIN-TUNNELING

MARTHA H. REDI, AND BERNARD S. GERSTMAN, *Department of Physics, Princeton University, Princeton, New Jersey 08544*
JOHN J. HOPFIELD, *Crellin Laboratory California Institute of Technology, Pasadena, California 91109*

ABSTRACT The spin-tunneling model of Hb—CO binding is used to calculate the binding rate at low temperature and high magnetic fields. The rate is calculated in second order perturbation theory assuming that spin-orbit coupling mediates the Hb iron electronic state change. The reaction which occurs at the crossing of the $S = 2$ and $S = 0$ energy vs. configuration coordinate curves is nonadiabatic, having a small electronic transition matrix element. Since detection of CO binding by polarized light in the Soret band makes it possible to observe hemes at specific orientation to the field direction, the rate is calculated for arbitrary heme orientation. Comparison with measurements at low temperature in zero field is made for spin quantization along the molecular crystal field direction.

INTRODUCTION

Much recent theoretical and experimental work has characterized quantum mechanical tunneling as a useful description of certain biochemical reactions. On the basis of the electronic spin-state change of the hemoglobin iron, we calculate the electronic contribution to the binding rate of carbon monoxide to hemoglobin and the electronic tunneling matrix element under high magnetic field conditions.

For myoglobin/hemoglobin (Mb/Hb)-ligand reactions as for electron transfer reactions involving cytochrome *c*, an electron tunneling process (1–3) determines the transition rate at all temperatures (4).

The size of the spin-orbit matrix element mediating the electronic spin change depends on the initial electronic spin state of the iron. This can be modified by attainable magnetic fields of 100 kGauss. The internal, local crystal field of the hemoglobin iron site defines a coordinate system for quantizing the spin of the iron. Application of an external magnetic field will affect the spin state of each iron, changing the size of the spin-orbit matrix element and hence the spin-tunneling rate. The overall recombination rate for CO will now depend on the orientation of each heme relative to the magnetic field. This will be reflected in a magnetic-field-induced anisotropy in the recombination rate of ligands. The calculations are carried out for a heme at arbitrary orientation to an external magnetic field and as a function of temperature and magnetic field strength.

Dr. Redi's present address is the Geophysical Fluid Dynamics Laboratory, Princeton University, Princeton, New Jersey 08544.

The hypothesis that spin tunneling regulates CO—Hb binding can be tested in detail. With polarized light monitoring the Soret absorption spectra, the rebinding of hemes at varying orientation to the magnetic field, H, can be measured and compared with theory (5). Experiments at the Massachusettes Institute of Technology National Magnet Laboratory (R. Austin and B. Gerstman) indicate the occurrence of an anisotropy induced by a magnetic field. Although we have not yet completed a detailed interpretation, these experiments indicate the significance of the physics being described here.

As shown by Jortner and Ulstrup (6) the nonadiabatic reaction rate for the CO-Hb (and electron transfer) reaction is separable into nuclear tunneling and electronic tunneling parts following the Born-Oppenheimer approximation. Nuclear tunneling characterized by a much smaller de Broglie wavelength only occurs at low temperature and is a spatial tunneling process. Electronic tunneling must be described by a quantum mechanistic state-to-state Landau-Zener tunneling transition. The electronic transition is a quantum process at all temperatures. We calculate the electronic contribution to the Hb-CO reaction rate. The molecular vibrational contribution has been investigated in detail by Jortner and Ulstrup (6).

Deoxy hemoglobin has spin $S = 2$, carbon monoxide has $S = 0$, and the bound CO—Hb complex also has $S = 0$. We consider the electronic states in the nuclear configuration at which $S = 0$ and $S = 2$ states have their lowest energy crossing. As carbon monoxide approaches the iron (Fig. 1) it destabilizes $S = 2$ and lowers the $S = 0$ level energy. When $S = 0$ is more energetically favorable than $S = 2$, a spin-tunneling transition via the $S = 1$ intermediate state can be effected by spin-orbit coupling (7). The small change in CO stretch frequency upon binding to Hb indicates that this chemical reaction is not accompanied by significant electron transfer and is governed by the spin-orbit interaction.

Stabilization of $S = 0$ is produced by the CO which allows increased electron delocalization and consequently a reduction of the exchange energy. The higher Coulomb energy of low spin states at $R_{CO} \rightarrow \infty$ is reflected in Hund's rule. Spin-orbit coupling is produced by the orbital motion of an electron, which causes it to perceive the nuclear electrostatic potential as a magnetic field. This effective magnetic field couples the electron's orbital angular momentum ℓ_i to its spin $\mathbf{s}_i$ with strength ξ adding a term to the Hamiltonian $\mathcal{H}' = \xi \Sigma_i \ell_i \cdot \mathbf{s}_i$. The spin-orbit

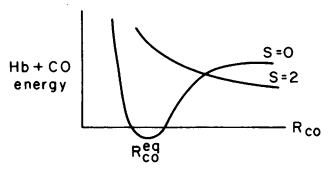

FIGURE 1

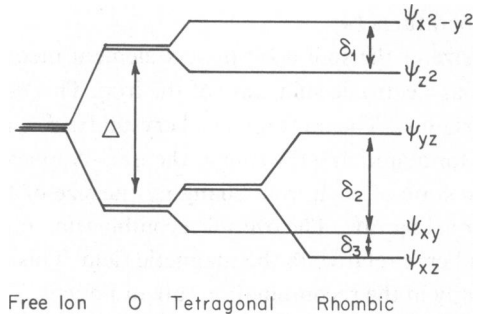

FIGURE 2

FIGURE 1 Energy vs. configuration coordinate diagram for two spin states of hemoglobin. R_{CO}^{eq} is the equilibrium separation distance between the iron and the carbon monoxide molecule.

FIGURE 2 Electronic structure of hemoglobin d orbital initial and final states.

interaction energy includes only the interaction of each spin with its own orbit since, in the many-electron atom, the central field is stronger than the interelectronic interaction.

From the Fermi Golden Rule of time-dependent perturbation theory, the transition probability per unit time, W_{ab}, from initial state $|a\rangle$ to final state $|b\rangle$ is given by

$$W_{ab} = \frac{2\pi}{\hbar} (V_{ab})^2 \rho(b)$$

where V_{ab} is the interaction matrix element effective in producing the electronic transition and $\rho(b)$, the density of final electronic states includes the effect of nuclear tunneling and the molecular vibration overlap factors. The matrix element which produces the spin-orbit-allowed tunneling transition through the intermediate states, $|j\rangle$, is

$$V_{ab} = \xi^2 \sum_j \frac{\langle b | \sum_i \ell_i \cdot \mathbf{s}_i | j \rangle \langle j | \sum_i \ell_i \cdot \mathbf{s}_i | a \rangle}{E_j - E_a}$$

where ξ is the spin-orbit coupling strength for a single 3d iron electron and $E_j - E_a$ is the energy difference between intermediate and initial states.

II. ELECTRONIC STRUCTURE OF Hb

In the Hb molecule, the free ferrous ion d-electron wave functions are not degenerate, but are shifted by the protein crystal field as in Fig. 2 (8).

The total orbital angular momentum L is equal to two but the z component of the total orbital angular momentum is not a good quantum number for the iron in Hb. The individual electronic wave functions can be characterized by components of angular momentum ($|m_\ell\rangle$) on the local molecular z axis, taken perpendicular to the heme plane (9).

$$\psi_{z^2} = |m_\ell = 0\rangle = \frac{K}{\sqrt{3}} [3\cos^2\theta - 1]$$

$$\psi_{x^2-y^2} = \frac{1}{\sqrt{2}} [|+2\rangle + |-2\rangle] = K \sin^2\theta \cos 2\phi$$

$$\psi_{yz} = \frac{1}{\sqrt{2}} [|+1\rangle - |-1\rangle] = K \sin 2\theta \sin\phi$$

$$\psi_{xz} = + \frac{1}{\sqrt{2}} [|+1\rangle + |-1\rangle] = K \sin 2\theta \cos\phi$$

$$\psi_{xy} = \frac{1}{\sqrt{2}} [|+2\rangle - |-2\rangle] = K \sin^2\theta \sin 2\phi, \; K^2 = \frac{15}{16\pi}.$$

The level ordering of Fig. 2 can be understood as follows. The crystal field symmetry at the iron in hemoglobin can be regarded as primarily octahedral (0) with axial (C_{4v}, D_{4h}) and rhombohedral (D_2) distortion. The symmetry of the full rotation group for the five degenerate free-ion valence states is reduced by the octahedral crystal field and further reduced by the axial and x-y distortions. Regarding the iron's ligands as centers of negatively charged

electron density, in 0 symmetry $\psi_{x^2-y^2}$ and ψ_{z^2} will have a larger repulsive Coulomb energy than ψ_{xy}, ψ_{yz} *and* ψ_{xz}, both sets being degenerate. An axial distortion which decreases the ligand electron density along the z axis will shift the ψ_{z^2} energy relative to $\psi_{x^2-y^2}$ and the energy of ψ_{xz} and ψ_{yz} relative to ψ_{xy}. A rhombohedral asymmetry removes the degeneracy of the xz and yz levels.

To determine the spin state of the iron we include the effects of spin-orbit coupling. This gives a spin Hamiltonian which breaks the fivefold degeneracy of the $S = 2$ state in iron in the absence of an external magnetic field (10). The perturbing Hamiltonian is

$$\mathcal{H}_{\mathbf{L}\cdot\mathbf{S}} = \lambda \mathbf{L} \cdot \mathbf{S}$$

where λ is the splitting parameter for a many-electron system. Carrying this perturbation to second order we get

$$\mathcal{H}_S = -\lambda^2 \sum_n \sum_{i,j=x,y,z} \frac{\langle o|L_i|n\rangle\langle n|L_j|o\rangle}{E_n - E_o} S_i S_j = -\lambda^2 \Lambda_{ij} S_i S_j$$

This can be written as $\mathcal{H}_S = DS_{z^2} + E(S_{x^2-y^2})$. Experimental values for D and E are given to be 5.3 and 0.9 cm^{-1}, respectively (11).

In a magnetic field the spin states are also affected by the Zeeman term and the full spin Hamiltonian is

$$\mathcal{H}_S = DS_{z^2} + E(S_{x^2} - S_{y^2}) + \beta g H M_s.$$

In presently attainable magnetic fields, the Zeeman and the zero-field splittings are approximately equal. The spin orbitals of the iron will therefore not be the individual M_s levels that they would be if the Zeeman term were operating alone in the absence of the zero-field splitting. Instead, the five-spin magnetic substates will be composed of combinations of M_s levels which are defined by using the external magnetic field's direction as the quantization axis. The overall tunneling matrix element will be the sum of the matrix elements of individual M_s values weighted by their probability for occupation which is determined by the probability amplitudes given by the spin-Hamiltonian and the Boltzmann temperature distribution.

Keeping this in mind, we compute the angular dependence of each M_s value separately (Sections IV and V) and show in Section VI how to combine the separate M_s matrix elements in a weighted sum to get the final matrix element, V_{ab}^2, which would be used in analyzing experimental data.

Referring to Fig. 2, $\Delta \sim 10^4 cm^{-1}$ (Weissbluth [8, p. 77]); δ_1, δ_2, and δ_3 are in the range of 10^2–$10^3 cm^{-1}$ (Weissbluth [8, p. 79]). The Zeeman splitting for $H = 10^5 G$, $\gamma M_L H_z \simeq 5\ cm^{-1} \ll \delta_i, \Delta$ so that H changes only the energy of the S_z sublevels; H does not mix orbital states.

Through the spin-orbit coupling perturbation we can rearrange the six ferrous iron electrons among the crystal field-shifted d levels while reducing the total spin S.

$$\ell \cdot \mathbf{s} = \ell_z s_z + \tfrac{1}{2}[\ell_+ s_- + \ell_- s_+].$$

Spin-orbit coupling is effective in changing the spin by only one unit of angular momentum at a time. Fig. 3 shows the different paths through which the $S = 0$ state can be reached from each initial sublevel of $S = 2$. For example, from $M_S = +2$ only $s_- s_-$, two lowering operations, can cause transition to $S = 0$.

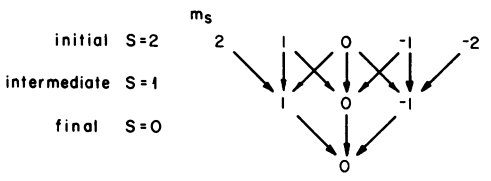

FIGURE 3

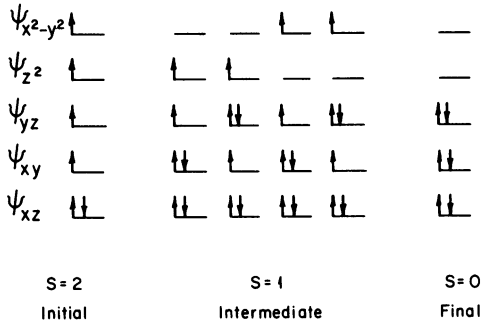

FIGURE 4

FIGURE 3 Transition paths in spin sublevel space for calculating Zeeman spin-transition matrix elements. Energy decreases to the right.

FIGURE 4 Occupation of d orbitals for hemoglobin initial, intermediate, and final electronic states.

Shown in Fig. 4 are the initial, final, and four intermediate states relevant to the $L \cdot S$ coupled spin transitions of the Hb—CO system. Because $|xz\rangle$, the lowest electron level (12, 13) is initially doubly occupied, we must calculate twelve transition moments of ℓ_i, one for each component of the electronic orbital angular momentum between the initial state and each intermediate state: $\langle xy|\ell_i|z^2\rangle$, $\langle xy|\ell_i|x^2-y^2\rangle$, $\langle yz|\ell_i|z^2\rangle$, $\langle yz|\ell_i|x^2-y^2\rangle$.

III. SPIN-ORBIT MATRIX ELEMENTS

Each state of the system is characterized by quantum numbers of total electron spin, (S, M_s) and by the occupation of particular electronic orbital angular momentum states $\{\ell_i\}$, $|\{\ell_i\}, S, M_s\rangle$. We need to compute

$$\xi(3d)\,\langle\{\ell_i\}', S', M_s'|\sum_i \ell_i \cdot \mathbf{s}_i|\{\ell_i\}, S, M_s\rangle.$$

This is equivalent to

$$\xi(3d)\sum_i \langle\{\ell_i\}'|\ell_i|\{\ell_i\}\rangle \cdot \langle S', M_s'|\mathbf{s}_i|S, M_s\rangle.$$

From the Wigner-Eckart theorem, the matrix elements of the individual electron-spin operator will be a product of a Clebsch-Gordon coefficient times the reduced matrix element of $\mathbf{s}_i$, $\langle S'\|\mathbf{s}_i\|S\rangle$ which is independent of M_s, M_s'.

The transitions are from $S = 2$ to $S = 1$ to $S = 0$. Between $S = 2$ and $S = 1$, the Wigner-Eckart theorem states that

$$\langle 1, M \pm 1|s_\pm^i|2, M\rangle = \pm S_{12}[(2 \mp M)(1 \mp M)]^{1/2}$$
$$\langle 1, M|s_z^i|2, M\rangle = S_{12}[(2 + M)(2 - M)]^{1/2}$$

and between $S = 1$ and $S = 0$

$$\langle 0, M \pm 1|s_\pm^i|1, M\rangle = \pm S_{10}[(1 \mp M)(\mp M)]^{1/2}$$
$$\langle 0, M|s_z^i|1, M\rangle = S_{10}[(1 + M)(1 - M)]^{1/2}$$

S_{12} and S_{10} are the reduced matrix elements $(1 \| \mathbf{s}_i \| 2)$ and $(0 \| \mathbf{s}_i \| 1)$. So between $S = 2$ and $S = 1$, referring to Fig. 3, the matrix elements will be

$$\begin{aligned}
\langle 1, 1 | s^i_- | 2, 2 \rangle &= -2\sqrt{3}\, S_{12} \\
\langle 1, 1 | s^i_z | 2, 1 \rangle &= \sqrt{3}\, S_{12} \\
\langle 1, 1 | s^i_+ | 2, 0 \rangle &= \sqrt{2}\, S_{12} \\
\langle 1, 0 | s^i_- | 2, 1 \rangle &= -\sqrt{6}\, S_{12} \\
\langle 1, -1 | s^i_- | 2, 0 \rangle &= -\sqrt{2}\, S_{12} \\
\langle 1, 0 | s^i_z | 2, 0 \rangle &= 2\, S_{12} \\
\langle 1, 0 | s^i_+ | 2, -1 \rangle &= \sqrt{6}\, S_{12} \\
\langle 1, -1 | s^i_z | 2, -1 \rangle &= \sqrt{3}\, S_{12} \\
\langle 1, -1 | s^i_+ | 2, -2 \rangle &= 2\sqrt{3}\, S_{12}
\end{aligned}$$

and between $S = 1$ and $S = 0$,

$$\begin{aligned}
\langle 0, 0 | s^i_- | 1, 1 \rangle &= -\sqrt{2}\, S_{10} \\
\langle 0, 0 | s^i_z | 1, 0 \rangle &= 1\, S_{10} \\
\langle 0, 0 | s^i_+ | 1, -1 \rangle &= \sqrt{2}\, S_{10}.
\end{aligned}$$

There will be several terms connecting $|a\rangle$ and $|b\rangle$ through a particular intermediate state (Fig. 4) since $\mathfrak{L}_i \cdot \mathbf{s}_i = \frac{1}{2}(\mathfrak{L}^i_+ s^i_- + \mathfrak{L}^i_- s^i_+) + \mathfrak{L}^i_z s^i_z$ is made up of three terms. The matrix elements of s^i_+, s^i_z are evaluated in the lab coordinate system. The external field **H** determines the z^L axis, with respect to which the iron spin is quantized. This is the coordinate system in which the $\mathfrak{L}_i \cdot \mathbf{s}_i$ raising and lowering operators are effective. $\mathfrak{L}^L_\pm$ and $\mathfrak{L}^L_z$ are the matrix elements for the transition from $|a\rangle$ to $|j\rangle$ in the laboratory coordinate system and in general are each made up of contributions from the matrix elements of $\mathfrak{L}^h_\pm$, $\mathfrak{L}^h_z \cdot \mathfrak{L}^h_\pm$ and $\mathfrak{L}^h_z$ are evaluated in the local molecular coordinate system at the heme, with coefficients given by the Euler rotation matrix (14) $A(\theta, \phi, \psi)$

$$\mathfrak{L}^L_i = \sum_{i=1}^{3} A_{ij}(\theta, \phi, \psi)\mathfrak{L}^h_j,$$

where A is found in Goldstein (15) equation 4–47. The transformation matrix A describes the contribution of each matrix element $(\mathfrak{L}^h_x, \mathfrak{L}^h_y, \mathfrak{L}^h_z)$ to each component $(\mathfrak{L}^L_x, \mathfrak{L}^L_y, \mathfrak{L}^L_z)$ in terms of the Euler angles θ, ϕ, ψ (Fig. 5) which specify the relative orientation of the two coordinate systems.

The axis z^h is in the direction of the heme normal and the x^h and y^h axes are in the plane of the heme through the pyrrole nitrogens. ϕ is the angle between x^L and the line "η" marking the intersection of the $x^h - y^h$ heme plane with the $x^L - y^L$ laboratory plane. ψ describes the rotation of the x^h, y^h axis in the heme plane about z^h and θ is the angle between the heme normal and the laboratory z^L axis. At the end of the calculation we average over angles in A since the hemoglobin monomers of the sample will be distributed among all possible orientations.

In the heme-coordinate system the individual electron angular momentum operators are in Table 6-1 of Brill (16).

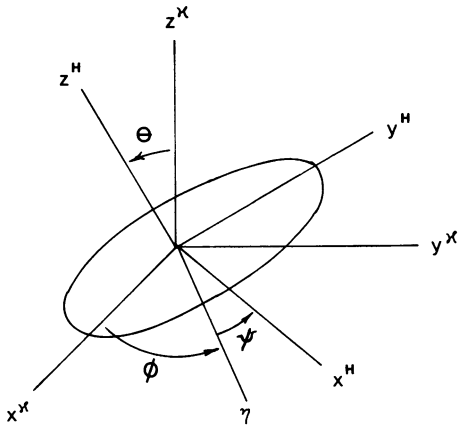

FIGURE 5 Relative orientation of heme (x^h, y^h, z^h) and laboratory (x^L, y^L, z^L) coordinate systems.

All orbital angular momentum matrix elements between $|z^2\rangle$ and $|xy\rangle$ are zero. Only the intermediate states formed by $\langle xy|\ell|x^2 - y^2\rangle$ or $\langle yz|\ell|z^2\rangle$ can produce a spin tunneling to $S = 0$. Only two intermediate states need be considered. Transforming to the laboratory coordinate system with $\ell^L = A \cdot \ell^h$

$$\begin{aligned}\langle xy|\ell_{\pm}^L|x^2 - y^2\rangle &= -2[A_{13} \pm iA_{23}]\\ \langle xy|\ell_z^L|x^2 - y^2\rangle &= 2A_{33}\\ \langle yz|\ell_{\pm}^L|z^2\rangle &= -\sqrt{3}\,[A_{11} \pm iA_{21}]\\ \langle yz|\ell_z^L|z^2\rangle &= -\sqrt{3}\,A_{31}.\end{aligned}$$

We will denote

$$\lambda_s^2 = \langle 2\|\mathbf{s}_i\|1\rangle\langle 1\|\mathbf{s}_i\|0\rangle\xi^2(3d) = \frac{\xi^2(3d)}{4\sqrt{3}},$$

where we evaluate the reduced matrix element in Appendix A. We will make the approximation that all energy denominators are equal to $E_j - E_a = E$; i.e., the orbital energy splittings of the $S = 2$ state are much less than the $S = 2$ to $S = 1$ energy difference. Breakdown of this approximation will change the contribution of each M_s term to the binding rate and will act to modify its angular dependence and magnitude. We have evaluated the spin-transition matrix elements and can now specify that the transition from $|2, \pm 2\rangle$ to $|0, 0\rangle$ through $|1, \pm 1\rangle$ is produced by the operator $T_{2,\pm 2} = (\lambda_s^2/4E)\,[2\sqrt{6}\ell_{\pm}^L\ell_{\pm}^L]$. For both transitions from $|2, \pm 1\rangle$ to $|0, 0\rangle$ there are two paths corresponding to a total perturbation $T_{\pm_1} = \mp\,(\lambda_s^2/E)\,\sqrt{6}\,\ell_{\pm}^L\ell_z^L$ and from $|2, 0\rangle$ to $|0, 0\rangle$ the three paths through intermediate states $|1, 1\rangle, |1, 0\rangle$ and $|1, -1\rangle$ produce a perturbation $T_0 = (\lambda_s^2/E)\,[2\ell_z^L\ell_z^L - \ell_+^L\ell_-^L]$. Each operator must be evaluated for all the possible intermediate states to compute $V_{ab}(M_s) = \Sigma_{\text{int.states}}\,T(M_s)$.

IV. RESULTS AND DISCUSSION OF HIGH-FIELD LIMIT

For each path in (S, M_s) space we sum the product of the spin and orbital momentum matrix elements over the two possible intermediate states of $\{\ell\}$. Contributions from all paths from

each initial $M_s = 2$ level are added. The square of the electronic tunneling matrix element from sublevel ($S = 2$, $M_s = \pm 2$) to ($S = 0$, $M_s = 0$) is

$$V_{ab}^2(\pm 2) = 6(2\sqrt{3})^2 \frac{\lambda_s^4}{E^2} |[A_{13} \pm iA_{23}][A_{11} \pm iA_{21}]|^2$$

$$= 6(2\sqrt{3})^2 \frac{\lambda_s^4}{E^2} \sin^2\theta[\cos^2\psi + \cos^2\theta \sin^2\psi], \tag{1}$$

from $M_s = \pm 1$

$$V_{ab}^2(\pm 1) = 6(2\sqrt{3})^2 \frac{\lambda_s^4}{E^2} |A_{33}[A_{11} \pm iA_{21}] + A_{31}[A_{13} \pm iA_{23}]|^2$$

$$= 6(2\sqrt{3})^2 \frac{\lambda_s^4}{E^2} (\cos^2\theta \cos^2\psi + \sin^2\psi \cos^2 2\theta), \tag{2}$$

from $M_s = 0$

$$V_{ab}^2(0) = 4(2\sqrt{3})^2 \frac{\lambda_s^4}{E^2} |[4A_{31}A_{33} - (A_{13} + iA_{23})(A_{11} - iA_{21}) - (A_{13} - iA_{23})(A_{11} + iA_{21})]|^2$$

$$= 4(2\sqrt{3})^2 \frac{\lambda_s^4}{E^2} 9 \sin^2\theta \cos^2\theta \sin^2\psi. \tag{3}$$

The angular dependence of the rebinding rates for each spin sublevel (Eqs. 1–3) is shown in Fig. 6. θ is the angle between heme normal and magnetic field direction and $\sin^2\psi$ and $\cos^2\psi$ have been averaged. All V_{ab}^2 (M_s) are independent of ϕ and at high temperature, if all levels are equally likely, the total electronic rate

$$\sum_{M_s} V_{ab}^2(M_s) = \left(\frac{\lambda_s^2}{E}\right)^2 144 = \frac{3\xi^4(3d)}{E^2}$$

is independent of θ, ϕ, ψ as expected.

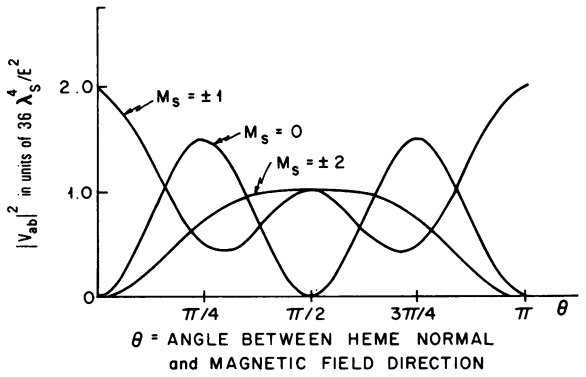

FIGURE 6 Spin orbit tunneling matrix element V_{ab}^2 for each spin sublevel.

At very low temperature we expect only $M_S = -2$ to be occupied initially. The sample will include hemes of all orientations. Averaging over heme rotation angle ψ, $V_{ab}^2(-2) = 36(\lambda_s^4/E)^2 \sin^2\theta(1 + \cos^2\theta)$. A sample of hemes with all z^h parallel to $\vec{H}$, ($\theta = 0$), will show no rebinding of CO for $H \gg 100$ kG. The magnitude of V_{ab} depends on the values of $\xi(3d)$ and E.

It is important to use $\xi(3d) = 400\ \text{cm}^{-1}$, the single electron spin-orbit coupling constant and not the term coupling constant $\xi(L, S) \simeq 100\ \text{cm}^{-1}$ for iron (14) in calculating $\lambda_s \sim 152\text{cm}^{-1}$.

The energy difference between initial and intermediate states, E, has contributions from three sources: the sum of occupied one electron energies, the exchange energy, and the magnetic field orientation energy. The last of these, the field-dependent energy difference, is small even for $H \sim 500$ kG.

$$E^H_{M_s=1} \simeq E^H_{M_s=2} \simeq 2\mu_B H \simeq 50\ \text{cm}^{-1}$$

and can be neglected.

Within the Hartree approximation, a sum of occupied one-electron energies for Fe^{+2} in the protein crystal field, will have lowest energy for the $S = 0$ configuration.

Exchange stabilizes $S = 2$ and $S = 1$ relative to $S = 0$ since the antisymmetrization of the wave function, to satisfy the Pauli Principle, reduces the interelectronic repulsion for states corresponding to larger values of S.

Loew and Kirchner (13) have shown for deoxy Hb how the porphyrin shifts the free ferrous ion $S = 1$ and $S = 2$ energy levels. They find that the free ferrous ion exchange energy differences $E^{ex}(S = 2) - E^{ex}(S = 1) = -4.4$ eV is reduced to about -3.0 eV for Fe^{+2} in model deoxy Hb. The sum over one-electron levels using the level separations of reference 17 in the myoglobin crystal field produces a configuration energy difference, which added to the ($S = 2$, $S = 1$) exchange energy difference, yields $E = 10{,}000\ \text{cm}-1$. Then for strong magnetic field conditions with covalency factor $\alpha^2 = 0.74$ (18)

$$V_{ab}(+2) = \frac{\xi^2(3d)\sqrt{3}}{E}\alpha^4 = 10\ \text{cm}^{-1} = 1.2 \times 10^{-3}\ \text{eV}.$$

The electronic spin-tunneling matrix element is a small parameter and satisfies the Landau-Zener non-adiabaticity condition (19) which can be written as,

$$K = \frac{2\pi |V_{ab}|^2}{\hbar\omega\sqrt{E_R K_B T}} < 1.$$

The values for the characteristic frequency of the system of $\hbar\omega \sim 100\ \text{cm}^{-1}$, and the transition induced reorganization energy of $E_R \sim 1000\ \text{cm}^{-1}$ are taken from Jortner and Ulstrup (6) but we use our own values of $V_{ab} \sim 10\ \text{cm}^{-1}$ and $T = 1.5$ K. This gives $K < 0.1$, consistent with CO binding being a nonadiabatic process. V_{ab} is about the same size as the tunneling matrix element effective in the electron transfer reaction of cytochrome c, which is typically about 10^{-3}–10^{-5} eV.

The role of the porphyrin in hemoglobin is to lower the energy of $S = 0$ and $S = 1$ relative to $S = 2$ through crystal field splitting, and to reduce the exchange energy. This makes the final state $S = 0$ more probable than in the free ferrous ion and decreases the energy denominator

E in V_{ab} so that spin-orbit coupling is a more effective perturbation in producing spin tunneling.

How crystal-field splitting prevents CO binding for a heme with $\theta = 0$ is most easily seen when the wave functions ψ_{xy}, etc., are expressed as a sum of components of $|m_\ell\rangle$. Transitions from $|z^2\rangle$ or $|x^2 - y^2\rangle$ to $|xy\rangle$ are not possible through ℓ_+ so that if only $M_s = -2$ is populated at low T, the spin cannot be lowered to $S = 0$ by spin-orbit coupling and carbon monoxide binding will not be observed for this orientation.

The spin-orbit interaction causes states which allow recombination to be mixed into the ground state. It is this d-level splitting which controls the low temperature rebinding rate of hemoglobin and carbon monoxide.

V. COMPARISON WITH ZERO MAGNETIC FIELD REBINDING RATE

Eqs. 1–3 can be used to interpret the zero-field Hb/CO recombination data obtained by Alberding et al. (20). The intrinsic molecular crystal fluid acts through an effective spin-Hamiltonian

$$\mathcal{H}_s = D S_y^2 + E (S_z^2 - S_x^2).$$

$D = 5.3$ cm^{-1} and $E = 0.9$ cm^{-1} were obtained by Nakano et al. (11) from paramagnetic susceptibility measurements for deoxy hemoglobin.

If the rhombic term proportional to E is neglected, the eigenvalues and eigenstates of the zero field Hamiltonian are shown in Fig. 7*a*. The quantization axis of Eqs. 1–3 has been taken to be the heme y-axis ($\psi = 0, \phi = \theta = \pi/2$). With $E = 0$, no rhombic splitting, only $M_s = \pm 2$ would exhibit spin-orbit allowed tunneling.

At temperatures below ~20°K the recombination rate would drop exponentially with temperature, with an activation energy corresponding to ~30°K, contrary to experiments. The discrepancy would not be eliminated by recent theoretical analysis of the Mossbauer data by Kent et al. (21) who suggest that the ground state may be ψ_{xy}. The inclusion of rhombic terms will mix the allowed tunneling state $M_s = -2$ into low-lying levels (Fig. 7*b*). The spin-tunneling model predicts a magnetic field-induced anisotropy for ψ_{xy} or ψ_{xz} lowest, but the details and sign of the anisotropy depends on which is lowest.

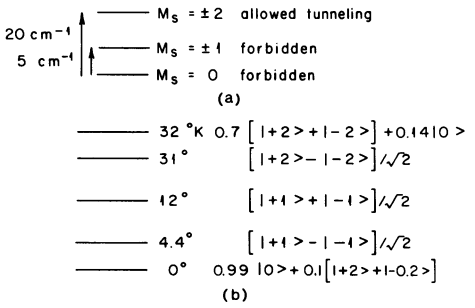

FIGURE 7 The eigenvalues and eigenstates of (*a*) $\mathcal{H}_S = DS_y^2$ and (b) $\mathcal{H}_S = DS_y^2 + E(S_Z^2 - S_X^2)$.

VI. DETECTION BY POLARIZATION ANISOTROPY

With the spin-Hamiltonian the spin system of the iron is composed of five sublevels which are combinations of M_s values:

$$\mathcal{H}_s \psi^i = E_i \psi^i \qquad i = 1\text{–}5$$

$$\psi^i = c^i_{+2}|+2\rangle + c^i_{+1}|+1\rangle + c^i_0|0\rangle + c^i_{-1}|-1\rangle + c^i_{-2}|-2\rangle$$

The states ψ^i are the eigenvectors of the spin-Hamiltonian $\mathcal{H}_s$. The transition rate W_{ab},

$$W_{ab} = F(T) \sum_{M_s} \frac{|V_{ab}(M_s)|^2 \sum_i |c^i_{M_s}|^2 e^{-E_i/KT}}{\sum_i e^{-E_i/KT}},$$

from initial state a to final state b is calculated by summing over each possible M_s. The matrix element for each M_s, $|V_{ab}(M_s)|^2$, has been calculated in section IV. The probability of occupying any M_s state $P(M_s)$ depends on the amplitude of that M_s state in each eigenstate ψ^i, weighted by the Boltzman probability for that eigenstate.

$$P(M_s, T, H) = \frac{\sum_{i=1,5} |c^i_{M_s}|^2 e^{-E_i/KT}}{\sum_{i=1,5} e^{-E_i/KT}}.$$

Here E_i is a function of the magnetic field strength and the zero field splitting parameters D and E. The temperature-dependent molecular vibrational factor $F(T)$ will be independent of M_s and H so that the CO binding rate will be

$$W_{ab}(T, H, \theta, \phi, \psi) = F(T) \sum_{M_s} P(M_s, T, H) V^2_{ab}(\theta, \phi, \psi, M_s)$$

for a heme of arbitrary orientation as a function of temperature and magnetic field strength.

W_{ab} is the rate constant $k(T, H, \theta, \phi, \psi)$ in the rate equation for the CO-Hb reaction

$$\frac{dN_{CO}}{dt} = k(N - N_{CO}),$$

N is the total number of hemes and N_{CO} is the number of hemes with CO bound. We neglect the Hb cooperativity and assume only Mb, protoheme or Hb monomers. Experiments by Alberding et al. (20) have shown that the equation above is not complete and that the solution

$$N_{CO}(t) = N(1 - e^{-kt})$$

must be replaced by

$$N_{CO}(t) = N \int dE g(E) \{1 - e^{-k(E)t}\}$$

where $g(E)$ and $k(E)$ are the normalized probability distribution of activation barriers, E,

and the corresponding rate constant for each, which are consistent with the observed function $N_{CO}(t)$.

The rate $k(E)$ is dependent on the total electronic-nuclear system energy. The energy dependence of $g(E)$ and $k(E)$ arises from conformational changes of the protein and will not depend on the electronic spin state of the iron. We set $k(E; T, H, \theta, \phi, \psi) = W_{ab}(E; T, H, \theta, \phi, \psi) = F(E; T) \Sigma_{M_s} P(M_s, T, H) V_{ab}^2 (\theta, \phi, \psi, M_s)$. We assume that $g(E)$ and $F(E; T)$ do not depend on M_s and are independent of (H, θ, ϕ, ψ). This approximation is unlikely to hold for binding studies of triplet O_2 at high H.

CO binding to hemes of specific orientation (θ, ϕ, ψ) can be detected by absorption of polarized light in the Soret band. Only light with polarization vector in the heme plane is absorbed. For a heme of arbitrary orientation the cross section for absorption of light polarized perpendicular to H is

$$\sigma_\perp(\theta, \phi, \psi) = \tfrac{1}{2} [\cos^2\phi + \sin^2\phi\cos^2\theta]$$

and for absorption of light polarized parallel to H

$$\sigma_\parallel (\theta, \phi, \psi) = \tfrac{1}{2} \sin^2\theta.$$

Thus the measured polarization absorption anisotropy as a function of H and T will be

$$\frac{A_{11} - A_\perp}{A_{11} + A_\perp}$$

where

$$A_{11}(T, H) = \langle \sigma_{11} (\theta, \phi, \psi) N_{CO}(T, H, \theta, \phi, \psi, t) \rangle_{\theta, \phi, \psi}$$
$$A_\perp (T, H) = \langle \sigma_1(\theta, \phi, \psi) N_{CO}(T, H, \theta, \phi, \psi, t) \rangle_{\theta, \phi, \psi}.$$

Thus, the number of hemes with CO bound as a function of time, temperature, magnetic field, and heme orientation in the laboratory magnetic field will be expressed by

$$N_{CO}(T, H, \theta, \phi, \psi, t) = N \int dE g(E) [1 - e^{-tW_{ab}(E;T,H,\theta,\phi,\psi)}],$$

This allows a quantitative optical anisotropy determination of the spin-tunneling theory of carbon monoxide binding to hemoglobin. The anisotropy results from the angular dependence in a magnetic field of W_{ab} due to the electronic spin transition which occurs during recombination.

APPENDIX A

The Reduced Matrix Elements $(1 \parallel \mathbf{s}_i \parallel 2)$ *and* $(0 \parallel \mathbf{s}_i \parallel 1)$

In Section IV we showed that the spin-tunneling matrix element V_{ab} is proportional to the product $(1 \parallel \mathbf{s}_i \parallel 2)(0 \parallel \mathbf{s}_i \parallel 1)$. These are matrix elements of individual electron s_i spin in the space described by the total spin S. For the coupling of four electron spins there are two configurations contributions to the normalized state vector of $S = 2$

$$|S = 2\rangle = \frac{1}{\sqrt{2}} [|s_{1\uparrow}\rangle |s_{2\uparrow}\rangle |s_{3\uparrow}\rangle |s_{4\uparrow}\rangle + |s_{1\downarrow}\rangle |s_{2\downarrow}\rangle |s_{3\downarrow}\rangle |s_{4\downarrow}\rangle].$$

There are eight configurations of up and down individual electron spins contributing to $|S = 1\rangle$

$$|S = 1\rangle = \frac{1}{\sqrt{8}}[|s_1\uparrow\rangle|s_2\uparrow\rangle|s_3\downarrow\rangle|s_4\uparrow\rangle + |s_1\uparrow\rangle|s_2\downarrow\rangle|s_3\uparrow\rangle|s_4\uparrow\rangle +$$
$$|s_1\uparrow\rangle|s_2\uparrow\rangle|s_3\uparrow\rangle|s_4\downarrow\rangle + |s_1\downarrow\rangle|s_2\uparrow\rangle|s_3\downarrow\rangle|s_4\uparrow\rangle +$$
$$|s_1\downarrow\rangle|s_2\downarrow\rangle|s_3\downarrow\rangle|s_4\uparrow\rangle + |s_1\downarrow\rangle|s_2\downarrow\rangle|s_3\uparrow\rangle|s_4\downarrow\rangle +$$
$$|s_1\downarrow\rangle|s_2\uparrow\rangle|s_3\downarrow\rangle|s_4\downarrow\rangle + |s_1\uparrow\rangle|s_2\downarrow\rangle|s_3\downarrow\rangle|s_4\downarrow\rangle].$$

An individual spin operator which can change M_{s_i} by $+1$ or -1 can transform $|S = 2\rangle$ to $|S = 1\rangle$ with amplitude $(1 \parallel \mathbf{s}_i \parallel 2) = \frac{1}{2}$. For the transition from $|S = 1\rangle$ to $|S = 0\rangle$, since

$$|S = 0\rangle = \frac{1}{\sqrt{6}}\{|s_{1\uparrow}\rangle|s_{2\uparrow}\rangle|s_{3\downarrow}\rangle|s_{4\downarrow}\rangle + |s_{1\uparrow}\rangle|s_{2\downarrow}\rangle|s_{3\uparrow}|s_{4\downarrow}$$
$$+ |s_{1\uparrow}\rangle|s_{2\downarrow}\rangle|s_{3\downarrow}\rangle|s_{4\uparrow}\rangle + |s_{1\downarrow}\rangle|s_{2\downarrow}\rangle|s_{3\uparrow}\rangle|s_{4\uparrow}\rangle$$
$$+ |s_{1\downarrow}\rangle|s_{2\uparrow}\rangle|s_{3\downarrow}\rangle|s_{4\uparrow}\rangle + |s_{1\downarrow}\rangle|s_{2\uparrow}\rangle|s_{3\uparrow}\rangle|s_{4\downarrow}\rangle\},$$
$$(0 \parallel \mathbf{s}_i \parallel 1) = \frac{1}{2\sqrt{3}}$$

so that $(S_{12}S_{10}) = 1/4\sqrt{3}$.

This research was supported by N.R.S.A grant 5F32-GM06184 to Dr. Redi and a National Science Foundation grant DMR 78-05916 to Drs. Hopfield and Gerstman.

Received for publication 17 September 1980 and in revised form 7 April 1981.

REFERENCES

1. Hopfield, J. J. 1974. Electron transfer between biological molecules by thermally activated tunneling. *Proc. Natl. Acad. Sci.* 71:3640.
2. Hopfield, J. J. 1977. Photoinduced charge transfer–critical test of mechanism and range of biological electron-transfer processes. *Biophys. J.* 18:311.
3. Redi, M. and J. J. Hopfield. 1980. Theory of thermal and photo-assisted electron tunneling. *J. Chem. Phys.* 72(12):6651.
4. Alben, J. O., D. Beece, S. F. Bowne, L. Eisenstein, H. Frauenfelder, D. Good, M. C. Marden, P. P. Moh, L. Reinisch, D. H. Reynolds, and K. T. Yue. 1980. Isotope effect in molecular tunneling. *Phys. Rev. Lett.* 44:1157.
5. Gerstman, B., R. Austin, J. J. Hopfield, R. Aggarwal, and M. Redi. Magnetically Induced Optical Anisotropy Measurements as a Test for Spin-Orbit Tunneling in Low Temperature Hemoglobin-CO Recombination, Federation Proceedings of American Societies for Experimental Biology, 39, 6, p. 1890, May 1, 1980.
6. Jortner, J., and J. Ulstrup. 1979. Dynamics of non-adiabatic atom transfer in biological systems. *J. Am. Chem. Soc.* 101(14):744.
7. Hopfield, J. J. 1979. Tunneling in Biological Systems. B. Chance, editor. Academic Press, Inc., New York. 646.
8. Weissbluth, M. 1974. Hemoglobin. Springer-Verlag, New York. 77.
9. Levine, J. N. 1974. Quantum Chemistry. Allyn and Bacon, Inc., Boston, Mass.
10. Pryce, M. A modified perturbation procedure for a problem in paramagnetism. *Proc. R. Soc. (Lond.) 63A*, 25 (1950).
11. Nakano, N., J. Otsuka, and A. Tasaki. 1972. Paramagnetic anisotropy measurements on a single crystal of deoxyhemoglobin. *Biochim. Biophys. Acta.* 278:355.

12. Olafson, B. D., and W. A. Goddard. 1977. Molecular description of dixoygen bonding in hemoglobin. *Proc. Natl. Acad. Sci.* 74(4):1315.
13. Loew, G. H., and R. F. Kirshner. 1978. Semiempirical calculations of model deoxyheme. *Biophys. J.* 22:179.
14. Tinkham, M. 1964. Group Theory and Quantum Mechanics. McGraw-Hill, New York.
15. Goldstein, H. 1950. Classical Mechanics. Addison-Wesley, Reading, Mass.
16. Brill, A. S. 1977. Transition Metals in Biochemistry. Springer-Verlag, New York.
17. Eicher, H., D. Bade, and F. Parak. 1976. Theoretical determination of the electronic structure and the spatial arrangement of ferrous ion in deoxygenated sperm whale myoglobin and human hemoglobin from Mössbauer experiments. *J. Chem. Phys.* 64:1446.
18. Huynh, B. H., G. C. Papefthymiou, C. S. Yeu, J. L. Groves, and C. S. Wu. 1974. Electronic structure of Fe^{2+} in normal human hemoglobin and its isolated subunits. *J. Chem. Phys.* 61:3750.
19. Zener, C. 1932. Non-adiabatic crossing of energy levels, *Proc. R. Soc (Lond.) A* 137:696.
20. Alberding, N., R. H. Austin, S. S. Chan, L. Eisenstein, H. Frauenfelder, J. C. Gunsalus, and T. M. Nordlund. 1976. Dynamics of carbon monoxide binding to protoheme. *J. Chem. Phys.* 65:4701.
21. Kent, T. A., K. Spartalian, and G. Lang. 1979. High magnetic field Mössbauer studies of deoxymyoglobin, deoxyhemoglobin, and synthetic analogues: theoretical interpretations. *J. Chem. Phys.* 71:4899.